Ultra-Reliable Communication Over Vulnerable All-Optical Networks Via Lightpath Diversity

Yonggang Wen, *Student Member, IEEE,* and Vincent W. S. Chan, *Fellow, IEEE*

Abstract—In this paper, we propose using spatial diversity via multiple node-disjointed lightpaths at the optical layer to achieve ultra-reliable communication with low delay between any source-destination pair in all-optical networks. Using a doubly stochastic point process model and a "genie-aided" receiver, we obtain an exponentially tight error probability bound for the lightpath diversity scheme under an independent lightpath failure model. Error probability of the proposed scheme can be designed to be significantly lower than that of a system without lightpath diversity, and system parameters (e.g., the number of lightpaths) can be optimized to achieve efficient utilization of a limited amount of transmitted optical energy. In particular, at the optimum operating point, each lightpath is allocated an optimum average number of signal photons per bit and is biased to have an effective error probability $2f$ if the decision is based on that path alone, where f is the lightpath failure probability. We also investigate the tradeoff between the error probability and the implementation complexity within the class of all "structured" receivers. We derive receiver architectures for both the optimal receiver, which has the best error performance but complicated receiver architecture, and the equal-gain-combining (EGC) receiver, which has suboptimum error performance but simpler receiver architecture. Closed-form error bounds for both receivers are obtained and compared with the "genie-aided" limit of the lightpath diversity scheme. Performance comparison shows that the simpler equal-gain-combing receiver provides similar performance as the optimal receiver in the regime of high signal-to-noise photon rate ratio ($\Omega = \lambda_s/M\lambda_n$, where λ_s/M is the signal photon rate per path, λ_n is the noise photon rate per path), and performs slightly worse than the optimal receiver in the low and medium signal-to-noise photon rate ratio regimes. It indicates that the simpler EGC receiver is preferred over the complicated optimum receiver in practical receiver design.

Index Terms—All-optical networks, doubly stochastic poisson process, lightpath diversity, network reliability.

I. INTRODUCTION

WHEN DEPLOYED, all-optical networks will trigger an architectural revolution for future broadband networks by eliminating all optical-to-electrical conversions along a lightpath [1], [2]. Originally proposed to exploit the huge bandwidth within the low attenuation transmission window of optical fibers to meet the exponential growth of traffic demand, optical networks have been evolved to provide other highly desirable features including wavelength switching, dynamic reconfigurability and improved reliability. These enhanced features can support highly reliable services that can transport, for instance, aircraft control signals between the cockpit and control surfaces over lightweight all-optical networks.

However, similar to other networks, all-optical networks are also vulnerable to different categories of failures. One kind of failure is physical component failure, for example, fiber cut and node hardware failure. Even if all network components are reliable individually, the communication between a source-destination pair can be interrupted by soft failures due to network problems, such as congestion, buffer overflow, and routing algorithm oscillations. In this paper, we focus on the problem of achieving ultrahigh reliability in all-optical networks for some special applications that may have to support services with super-high data rates and/or critical time deadlines.

To support ultra-reliable communication in all-optical networks, two mechanisms can be used to counteract the aforementioned failures: protection-switching and simultaneous lightpath-diversity. Currently, the prevailing approach is the protection-switching scheme, as implemented commercially in Synchronous Optical Network (SONET)-based networks. In this scheme, if a source-destination communication session is interrupted by a failure, a detection algorithm first identifies the failure, and then communication is switched to another dedicated or shared backup connection. However, this protection-switching mechanism can induce a rather long delay ($\sim$ 50-ms restoration time, a SONET standard [3]). Thus, this scheme is inappropriate for some unique applications. For example, considering the service with super-high data rate ($>$10 Gb/s), a short-time interruption can result in a large amount of data loss. In other critical applications (e.g., when the network is used for transporting control signals between the cockpit and control surfaces in an aircraft), the time-deadline of control-message delivery needs to be shorter than 1 ms and probably ten times faster in failure detection. This is faster than the speed at which most optical components can switch and protection-switching protocol can be executed. For such applications, instead of increasing the speed of failure detection and lightpath switching to meet increasing data rates and critical time deadlines, multiple-path diversity is a better alternative that can be implemented with current technologies. Chan and Parikh have explored this mechanism in [4] and [5]. In that work, they looked at a joint data link control layer and transport layer reliable message delivery scheme and have found significant merit for using path diversity efficiently via error correction coding techniques. In this paper, we extend their work to a physical-layer lightpath diversity mechanism, using an optimum signaling and detection scheme to optimize system performance and provide reliable end-to-end data delivery in the presence of failures (e.g., fiber cuts and node hardware failures).

The advantages of the proposed reliable transmission scheme, which is based on spatial diversity via multiple disjoint lightpaths belonging to different shared-risk groups, are at least twofold. First, because the entire mechanism is implemented at the physical layer, it provides a much faster response to failures than protocols that provide end-to-end reliability at higher layers, such as the transmission control protocol (TCP) at the transport layer. Second, as will be shown in this paper, the symbol error probability of multiple-lightpath transmission is significantly lower than that of single-lightpath transmission in medium and high signal-to-noise photon rate ratio regimes. In particular, for a source-destination pair connected by M lightpaths, the symbol error probability in the high signal-to-noise photon rate ratio regime is asymptotically equal to $\prod_{i=1}^{M} f_i$ (f_i is the failure probability of the ith lightpath.) This is the asymptotic reliability limit of the multiple-lightpath transmission scheme. By choosing the number of lightpaths used, this limit can be made arbitrarily small compared with the asymptotic symbol error probability of using only a single lightpath between a source-destination pair.

Compared with the single lightpath transmission, one major disadvantage of the lightpath diversity scheme is that the same message is sent repeatedly through a group of disjointed lightpaths and, thus, degrades the throughput per channel use by a factor of M for an M-connected source-destination pair. However, in order to achieve ultra-reliable communication with low delay, for example, in an aircraft control network, we choose to sacrifice some bandwidth efficiency for reliability in a bandwidth-rich environment. In fact, multiple connections between any source-destination pair are necessary for reliable networks [6], and both parallel signaling and sequential signaling over multiple connections can realize high reliability. The lightpath diversity scheme satisfies this necessary condition by splitting each channel symbol and sending the fragments simultaneously through M disjointed lightpaths. Another potential disadvantage of a lightpath diversity scheme is that more energy may have to be used than a single lightpath scheme. However, the error probability of any single lightpath scheme is bounded from below by the lightpath failure probability f. In order to achieve an error probability below f, it is necessary to use more than one lightpath to lower the asymptotic error limit. In this work, using optimum signaling and detection, we choose the number of lightpaths to optimize energy efficiency and reduce the amount of additional necessary optical energy to the minimum.

We investigate the proposed ultra-reliable transmission mechanism from both a theoretical and an engineering perspective. From the theoretical perspective, we characterize and optimize the error performance of the lightpath diversity system. From the engineering perspective, we develop a class of structured receivers and evaluate their error performance. The remainder of the paper is organized as follows. In Section II, we formulate the detection problem and introduce the structured receiver architecture. We characterize the error probability of the lightpath-diversity system via an idealized receiver in Section III. This benchmark result is called the "genie-aided" receiver limit which is a lower bound for practical receivers. In Section IV, the system is optimized via: 1) minimizing the error probability for a given amount of optical energy
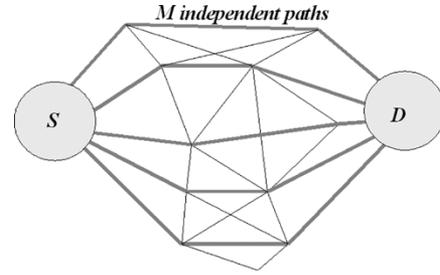
Fig. 1.　Network model for an M-connected source-destination pair in a densely connected all-optical network.
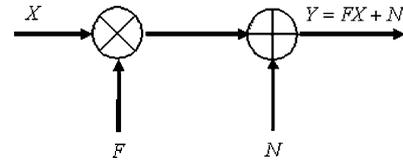
Fig. 2.　Discrete channel model of an individual lightpath. X is the input, Y is the output, F is a Bernoulli random variable indicating the lightpath state, and N is the noise.

and 2) minimizing the total optical energy for a target error probability. In Section V, we illustrate the tradeoff between implementation complexity and error performance in the receiver design. Also, in this section, the architecture of the optimal receiver is derived, and its error probability bound is obtained and compared with the "genie-aided" receiver limit. One suboptimal receiver, the equal-gain-combining (EGC) receiver, is developed in Section VII. Its error probability bound is also calculated and compared with the "genie-aided" receiver limit.

II. PROBLEM FORMULATION

A. Network Model

We assume that the physical topology of the optical network has dense enough connections such that M node-disjointed lightpaths can always be found between some source-destination pair, as shown in Fig. 1 [6], [7]. All the lightpaths must belong to different shared-risk groups to justify the following independent failure model. Each lightpath can be modeled as a discrete additive-noise channel with UP and DOWN states. In particular, for the ith lightpath, the DOWN state corresponds to a disconnected lightpath and occurs with probability f_i, and the UP state occurs with probability $1 - f_i$ and corresponds to a viable lightpath. Mathematically, the input–output relation of the channel can be expressed as $Y_i = F_i X_i + N_i$, as shown in Fig. 2, where X_i and Y_i are the input and output, F_i is the lightpath state indicator function which is a Bernoulli random variable with $\Pr(F_i = 0) = f_i$ and $\Pr(F_i = 1) = 1 - f_i$, and N_i is the additive noise (zero if no optical amplifier is used). For a given source-destination pair, we define a lightpath state vector $\mathbf{F} = (F_1, F_2, \ldots, F_M)^T$, where each component F_i is an independent Bernoulli random variable. The source-destination pair is also characterized by a delay vector $\boldsymbol{\tau} = (\tau_1, \tau_2, \ldots, \tau_M)^T$, where each component τ_i is the delay of the ith lightpath, an attenuation vector $\mathbf{L} = (l_1, l_2, \ldots, l_M)^T$, where each component l_i is the attenuation of the ith lightpath,
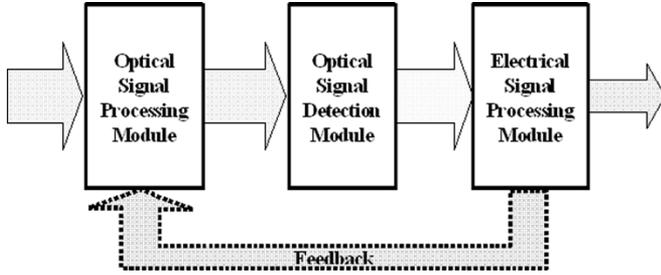
Fig. 3. Structured receiver architecture. It is divided into three cascaded modules: an optical signal processing module, an optical detection module, and an electrical signal processing module.

and a noise vector $\mathbf{N} = (N_1, N_2, \ldots, N_M)^T$, where each component N_i is the noise of the ith lightpath.

In this paper, binary pulse-position modulation (BPPM) is used to simplify the receiver implementation by not having to adaptively set the decision threshold as in the case of on–off-keying (OOK) modulation. The modulated signal is split into M parts. Each part is sent over an independent lightpath to the receiver. At the destination node, the received optical signals are either combined optically before detection, or individually detected and electrically combined for symbol-by-symbol decisions.

With a photon-counting receiver, the photo-event count at the receiver's output obeys Poisson statistics [8] if the optical signal is generated by a single-mode laser. The expected photo-event arrival rate λ (the mean number of photo-event per unit time) is determined by the received optical power (i.e., energy per bit, given the bit rate). In our work, the received optical power is a random variable due to the random channel model as illustrated in Fig. 2. Thus, the photo-event process at the detector output can be modeled by a doubly stochastic point process [9].

B. Structured Receiver Architecture

We can design an optical receiver using two different approaches. Due to the quantum nature of weak optical signals, one approach is to use a full quantum description of the receiver, and optimize it over the class of physically realizable measurements [10]. Quantum receivers are optimum in energy efficiency. However, they are complicated and hard to realize with current electrical and optical components. In this paper, we take a "structured" or "semi-classical" approach [11]. Although structured receivers suffer a 3-dB loss of energy efficiency over optimum receivers for binary signaling, they are much simpler and easier to implement with current technologies. The architecture of all possible structured receivers can be divided into three cascaded processing modules, as illustrated in Fig. 3: an optical signal processing module, an optical detection module, and an electrical signal processing module. The three modules must be jointly optimized to achieve a globally optimum performance. Causal feedbacks among these blocks are also permissible, which can make structured receivers achieve the quantum limit for binary signaling [15]. However, due to their complexity, we will not consider them here.

III. SYSTEM CHARACTERIZATIONS

In this section, we characterize the symbol error probability of the lightpath-diversity scheme with an exponentially tight upper bound. We assume that, at the destination node, an idealized receiver obtains the lightpath state vector $\mathbf{F}$ from a "genie" (i.e., the receiver has information of the channel states.) At the optical signal processing module, optical delay lines are used to compensate for delay variations among different lightpaths (fiber delays can also be replaced by time delays in the electrical signal processing stage if M parallel detectors are used.) At the optical detection module, the photo-events at the output of the M detectors are recorded for symbol decisions. At the electrical processing module, we apply the maximal-likelihood (ML) decision rule to the vector output of the detectors to make optimal symbol-by-symbol decisions.

Under the general network model given in Section II-A, the optimum receiver is complex. The analysis and results would not provide much insight into the signaling and detection schemes due to the heterogeneity of individual lightpath. Here, we make the simplifying assumption of homogeneous lightpaths, resulting in a simpler derivation and the results will provide much better insight into the proposed transmission scheme.

1) *All lightpaths are assumed to be homogeneous and independent; i.e.,* $f_1 = f_2 = \cdots f_M = f$ *and* $N_1 = N_2 = \cdots N_M$. Although some generality is lost due to this assumption, results based on this assumption will provide better insight for the optimization of the proposed transmission scheme. Under this assumption, a uniform energy (per bit) allocation algorithm at the transmitter is optimal (see Appendix A). Otherwise, the optimal energy (per bit) allocation algorithm can be obtained by solving a complicated convex optimization problem.

2) *All attenuation parameters are assumed to be equal and normalized to one.* Note that this result can be generalized to the unequal attenuation case by solving a complicated convex optimization problem.

A. Photo-Event Counting Process

With the BPPM signaling and the uniform energy (per bit) allocation, the optical signal power over the ith lightpath is either

$$P_i^{(0)}(t) = \begin{cases} \frac{P_s}{M}, & 0 \le t \le \frac{T}{2} \\ 0, & \frac{T}{2} \le t \le T \end{cases} \tag{1a}$$

for hypothesis H_0 (i.e., symbol "0"), or

$$P_i^{(1)}(t) = \begin{cases} 0, & 0 \le t \le \frac{T}{2} \\ \frac{P_s}{M}, & \frac{T}{2} \le t \le T \end{cases} \tag{1b}$$

for hypothesis H_1 (i.e., symbol "1"). In both cases, P_s is the average output power of the laser, and T is the symbol time.

The received optical signals can be corrupted by amplifier noises if optical amplifiers are used. We assume that the noise process receives contributions from many spatial-temporal modes, and the probability of two successive noise-driven photo-events coming from the same spatial-temporal mode is close to zero. It follows that the Weak Photon-Coherence Assumption holds, and we can approximate the noise-driven
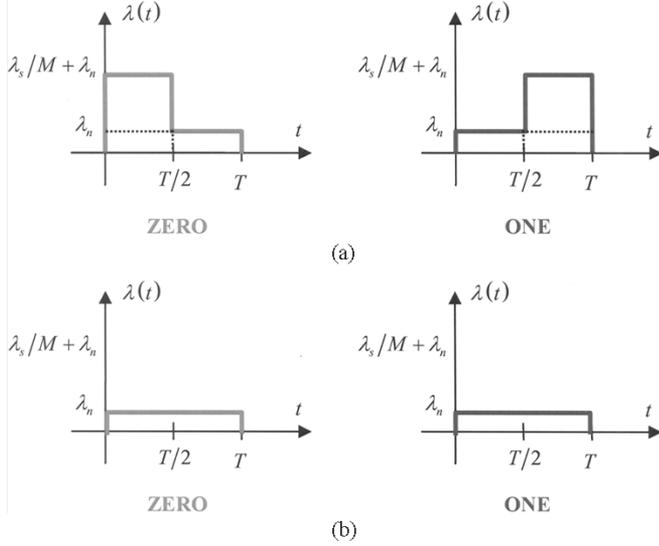
Fig. 4. Detected photo-event rates for two hypotheses with BPPM signaling. (a) When the lightpath is UP, the detected rate is the sum of the signal rate and the noise rate. (b) When the lightpath is DOWN, the detected rate is only the noise rate.

photo-event process with a point process of a constant rate λ_n equal to its mean [16]. This approximation is accurate within about 1 dB for a single channel. With M channels and many amplifiers in cascade, we expect the approximation to be even better. Consequently, taking into account of the noise, the photo-event rate at the output of the ith detector is either

$$\lambda_i^{(0)}(t) = \begin{cases} \frac{F_i \lambda_s}{M} + \lambda_n, & 0 \leq t \leq \frac{T}{2} \\ \lambda_n, & \frac{T}{2} \leq t \leq T \end{cases} \quad (2a)$$

for hypothesis H_0, or

$$\lambda_i^{(1)}(t) = \begin{cases} \lambda_n, & 0 \leq t \leq \frac{T}{2} \\ \frac{F_i \lambda_s}{M} + \lambda_n, & \frac{T}{2} \leq t \leq T \end{cases} \quad (2b)$$

for hypothesis H_1. In both cases, $\lambda_s = \eta P_s / h\nu$ (η is the quantum efficiency of the detector, $h\nu$ is the photon energy) is the rate of the signal photo-event process with an average signal power of P_s, and F_i is a Bernoulli random variable with parameter $1 - f$. Fig. 4 shows the rates of the photo-event counting process for a) $F_i = 1$ and b) $F_i = 0$. For a given hypothesis, the photo-event process is a doubly stochastic point process due to its random rate parameter.

B. Optimum Decision Rule

If $m \leq M$ lightpaths are UP during the symbol duration, we can re-index them from 1 to m for a "genie-aided" receiver. Under this scenario, the optimal decision rule is the same as the detection rule for the scenario with m perfectly reliable lightpaths [12], i.e.,

$$\sum_{i=1}^{m} k_{i1} \underset{\widehat{H}=H_1}{\overset{\widehat{H}=H_0}{\underset{<}{\gtrless}}} \sum_{i=1}^{m} k_{i2} \quad (3)$$

where k_{i1} and k_{i2} are photo-event counts during $[0, T/2]$ and $[T/2, T]$ over the ith lightpath, respectively.

C. Error Probability Upper Bound

In this section, we derive an exponentially tight upper bound for the error probability of the "genie-aided" receiver via a two-step procedure: 1) the Chernoff bound of the error probability conditioning on the number of UP lightpaths is calculated and 2) the overall error probability upper bound is calculated by averaging the conditional error probability bound over the distribution of the number of UP lightpaths.

Given that m lightpaths are UP during the transmission, the conditional error probability is defined as

$$\Pr(\varepsilon|m) = p_0 \Pr\left[\sum_{i=1}^{m} k_{i1} \leq \sum_{i=1}^{m} k_{i2}|H_0, m\right]$$
$$+ p_1 \Pr\left[\sum_{i=1}^{m} k_{i1} \geq \sum_{i=1}^{m} k_{i2}|H_1, m\right]$$
$$= \Pr\left[\sum_{i=1}^{m} k_{i1} \leq \sum_{i=1}^{m} k_{i2}|H_0, m\right] \quad (4)$$

where p_0, p_1 are probabilities of sending the "ZERO" or "ONE" bit, and the second equality is due to the symmetry of binary pulse-position modulation and $p_0 = p_1 = 1/2$ for equiprobable digital source. Since the closed form solution of $\Pr(\varepsilon|m)$ is involved with summation of infinite numbers of terms, we focus on the exponentially tight Chernoff upper bound [12]

$$\Pr\left[\sum_{i=1}^{m} k_{i1} \leq \sum_{i=1}^{m} k_{i2}|H_0, m\right]$$
$$\leq E_{s>0}\left\{ e^{s\left(\sum_{i=1}^{m} k_{i2} - \sum_{i=1}^{m} k_{i1}\right)} |H_0, m \right\}$$
$$= \exp\left\{ mN_n(e^s - 1) + \left(\frac{mN_s}{M} + mN_n\right)(e^{-s} - 1)\right\} \quad (5)$$

where $N_s = T\lambda_s/2$ is the average data-driven photo-event count of duration $T/2$ with binary pulse-position modulation and $N_n = T\lambda_n/2$ is the average noise-driven photo-event count per 1/2 bit. Since the inequality is valid for any value of $s > 0$, the bound can be tightened by minimizing the right-hand side of (5)

$$\Pr(\varepsilon|m) \leq \min_{s>0} \exp\left\{ mN_n(e^s - 1) + \left(\frac{mN_s}{M} + mN_n\right)(e^{-s} - 1)\right\}$$
$$= \exp\left\{ -m\left(\sqrt{\frac{N_s}{M} + N_n} - \sqrt{N_n}\right)^2\right\} \quad (6)$$

where the minimum is achieved when $e^s = \sqrt{1 + N_s/(MN_n)}$.

The overall error probability is then obtained by averaging the conditional error probability (6) over the distribution of the number of UP lightpaths m

$$\Pr(\varepsilon) = \sum_{m=0}^{M} \Pr(\varepsilon|m)\Pr(m). \quad (7)$$

The number of UP lightpaths can be written as $m = \sum_{i=1}^{M} F_i$. It can be verified that m has a binomial distribution of

$$\Pr(m) = \frac{M!}{m!\,(M-m)!}\,(1-f)^m\,f^{M-m}. \qquad (8)$$

Substituting (6) and (8) into (7), we obtain

$$\Pr(\varepsilon) \leq \sum_{m=0}^{M} \frac{M!}{m!\,(M-m)!}\,(1-f)^m\,f^{M-m}e^{-m\psi(N_s,N_n,M)}$$
$$\triangleq \mathrm{PB_{GA}} \qquad (9)$$

where $\psi(N_s,N_n,M) = \left(\sqrt{N_s/M + N_n} - \sqrt{N_n}\right)^2$. Note that the right-hand side of (9) has the form of the characteristic function of the random variable m. Using the fact that the characteristic function of a binomial random variable $X \sim B(n, 1-f)$ is $(f + (1-f)e^{jv})^n$ [13], we obtain the upper bound of the overall error probability as

$$\mathrm{PB_{GA}} = \left[f + (1-f)e^{-\left(\sqrt{(N_s/M)+N_n}-\sqrt{N_n}\right)^2} \right]^M. \qquad (10)$$

For a sanity check, if $f = 0$, (10) turns out to be

$$\mathrm{PB_{GA}} = \exp\left\{ -\left(\sqrt{N_s + MN_n} - \sqrt{MN_n}\right)^2 \right\} \qquad (11)$$

which is the error probability bound for the source-destination pair connected by M reliable lightpaths. Note that f is the probability of the lightpath being DOWN, where the error probability is equal to 1, and $1 - f$ is the probability of the lightpath being UP, where the error probability is bounded by the term $e^{-\psi(N_s,N_n,M)}$, which is the Chernoff bound for the error probability of a single lightpath with N_s/M signal photons per bit and N_n noise photons per 1/2 bit. It follows that the term $f + (1-f)\exp\{-\psi(N_s,N_n,M)\}$ is the Chernoff bound of the expected error probability for a single lightpath with failure probability f. The overall error probability bound is obtained by reducing this expected error probability of a single lightpath to its Mth power, which can be defined as the lightpath diversity gain.

The error probability upper bound (10) is plotted in Fig. 5, where the error curves exhibit different characteristics in three different signal-to-noise photon rate ratio regimes.

In the low signal-to-noise photon rate ratio regime, the lightpath-diversity mechanism has an inherently poor error performance and, thus, is of no engineering interest. In particular, if we let $f \to 0$ and $\Omega = N_s/(M \cdot N_n) \ll 1$, the error probability bound is reduced to

$$\mathrm{PB_{GA}} \approx \exp\left\{ -\frac{N_s^2}{4MN_n} \right\}. \qquad (12)$$

The error exponent decreases if we use more lightpaths, which suggests that it actually hurts to use lightpath diversity in the low signal-to-noise photon rate ratio regime.

In the high signal-to-noise photon rate ratio regime, the error probability curves converge to error floors because the effect of lightpath failures dominates that of the amplification and detection noises. In fact, if we let $N_s/M \to \infty$ and $N_s/M \gg N_n$ for a fixed f, we obtain

$$\mathrm{PB_{GA}} \approx f^M. \qquad (13)$$
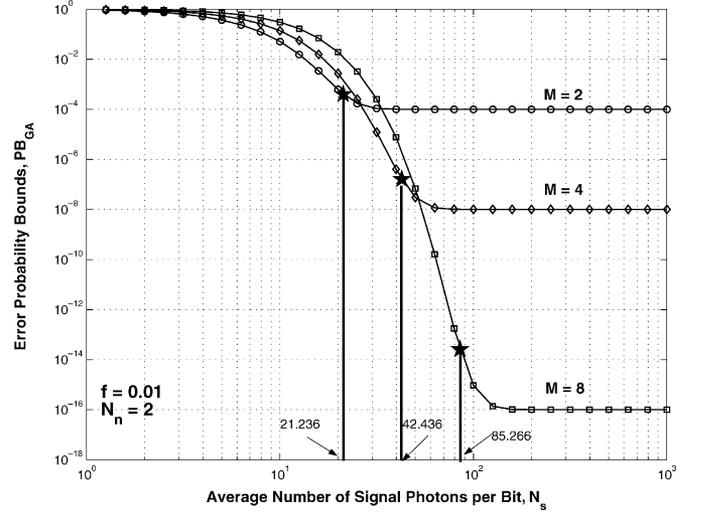
Fig. 5. Error probability bounds for the idealized receiver with different number of lightpaths. $f = 0.01$ and $N_n = 2$.

This verifies that the error floor phenomenon corresponds to the event in which the source-destination pair is disconnected from each other, with probability of f^M. This result suggests that topologies with a small probability of disconnection are preferable for reliable networks [6], [7]. Moreover, due to this saturation property, we cannot improve the error performance by simply increasing the signal-to-noise photon rate ratio. Thus, it is inefficient in energy utilization to work in the super-high signal-to-noise photon rate ratio regime.

In the medium-to-high signal-to-noise photon rate ratio regime, the error performance depends on the number of lightpaths (M, the lightpath diversity gain) and the signal-to-noise photon rate ratio. After some algebraic manipulations, (10) can be written as

$$\mathrm{PB_{GA}} = \left\{ f + (1-f)\exp\left[-N_n\left(\sqrt{\Omega+1} - 1\right)^2 \right] \right\}^M \qquad (14)$$

where the signal-to-noise photon rate ratio is given by $\Omega = N_s/MN_n$. As shown in (14), in order to achieve a lower error probability, we want to increase the number of lightpaths M and the signal-to-noise photon rate ratio simultaneously. However, for a given amount of optical energy per bit (signal photons per bit, N_s), we have

$$M \times \Omega = \frac{N_s}{N_n}. \qquad (15)$$

This indicates that the number of lightpaths M and the signal-to-noise photon rate ratio Ω are two factors competing for a limited amount of optical energy. Therefore, we need to balance this tradeoff to optimize the system performance and improve the energy efficiency, which will be addressed in the next section.

IV. System Optimizations

The output energy (per bit) of the transmitter is limited by physical constraints such as laser construction. We need to utilize this limited amount of optical energy efficiently. As indicated in last section, the energy efficiency can be improved over
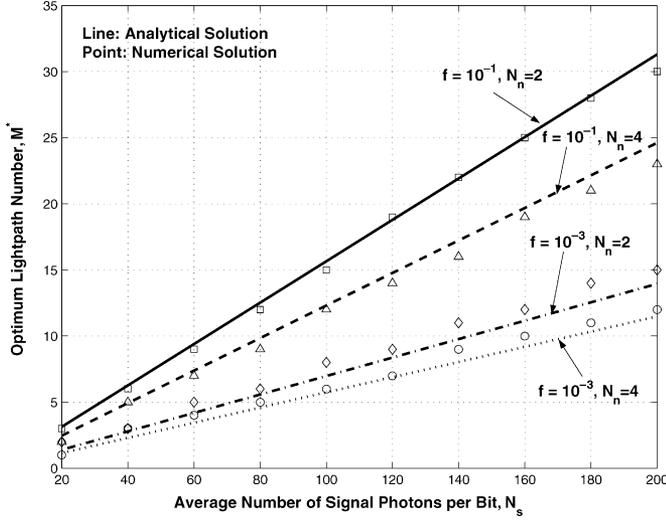
Fig. 6. Optimal number of lightpaths M^* is plotted against the average number of signal photons per bit N_s. As a comparison, we also plot the results from the exhaustive search algorithm.

the choice of the number of lightpaths for different objective functions.

A. Minimizing the Error Probability Bound ($\mathrm{PB_{GA}}$) for a Limited Amount of Optical Energy (N_s)

Given a limited amount of optical energy, the number of lightpaths can be chosen to minimize the error probability. Equivalently, we can minimize the error probability bound $\mathrm{PB_{GA}}$ since this bound is exponentially tight. We formulate it as the following nonlinear programming problem:

$$\min \quad G(M) = \left(f + (1-f) e^{-\psi(N_s, N_n, M)} \right)^M$$
$$\text{s.t.} \quad M \in \mathbb{N} \text{ (the set of positive integers)}. \quad (16)$$

Instead of finding the exact solution, we relax the integer constraint, and assume M is a positive real number to solve the approximate problem without the integer constraint. Note that the minimum of $G(M)$ without the integer constraint is a lower bound of the minimum of $G(M)$ with the integer constraint. If $0 < f < 1/2$ (we are interested in this region since practical networks seldom have $f > 1/2$), the optimum lightpath number M^* (see Appendix B) is approximated by

$$M^* \approx \frac{N_s}{\zeta(f, N_n)} \quad (17)$$

where $\zeta(f, N_n) = \ln(1/f - 1) + 2\sqrt{N_n}\sqrt{\ln(1/f - 1)}$. For comparison, we have also found the optimal integer M^* by using an exhaustive search algorithm. In Fig. 6, the results from both the exhaustive search algorithm (bullets) and the analytical solution (lines) are plotted against different signal energy levels, i.e., the average number of signal photons per bit N_s. The analytical results match the numerical results well.

According to (17) and Fig. 6, the optimum lightpath number M^* decreases with higher noise energy per slot since we want to maintain a certain level of signal-to-noise photon rate ratio, and also decreases with more reliable lightpaths since we have no incentive of using lightpath diversity if the lightpath is reliable. Moreover, the optimum lightpath number M^* increases

linearly with the transmitted energy N_s per bit. This suggests that each lightpath requires a fixed optimal average number of signal photons

$$\frac{N_s}{M^*} = \ln\left(\frac{1}{f} - 1\right) + 2\sqrt{N_n}\sqrt{\ln\left(\frac{1}{f} - 1\right)} \quad (18)$$

per bit, which is fully determined by the parameters of the lightpath, i.e., the lightpath failure probability f and the noise level N_n. When the lightpath is very reliable (i.e., $f \ll 1$), this number is asymptotically equal to $-\ln(f) + 2\sqrt{N_n}\sqrt{-\ln(f)}$. This asymptotic result suggests that the optimal average number of photons per lightpath increases with higher noises and more reliable lightpaths. This is because, under these two scenarios, we need more optical energy per lightpath to bias the lightpath at the optimum operating point, which will be addressed next.

Substituting (17) into (10), the minimum error probability bound is approximated by

$$\mathrm{PB_{GA}^*} \approx (2f)^{M^*}. \quad (19)$$

This indicates that, at the optimum operating point where the number of lightpaths are optimally chosen to minimize the error probability bound for a given amount of optical energy (per bit), each lightpath is biased to have an effective error probability of $2f$, which is close to the saturation error probability of f for an individual lightpath. This result implies that the optimum operating point lies in the medium-to-high signal-to-noise photon rate ratio regime but near the high signal-to-noise photon rate ratio regime. This also justifies why each lightpath requires more photons when the lightpath is more reliable. In fact, when the lightpath failure probability f decreases, we need to increase the signal-to-noise photon rate ratio to sustain an effective error probability of $2f$.

Furthermore, if $f \ll 1$, the minimum error probability bound is approximated by

$$\mathrm{PB_{GA}^*} \approx \exp\left\{ -\frac{1}{1 + 2\sqrt{-\frac{N_n}{\ln(f)}}} N_s \right\}. \quad (20)$$

The error exponent decreases linearly with the optical energy (per bit). This again suggests that the optimum strategy works at the medium-to-high signal-to-noise photon rate ratio regime and near the high signal-to-noise photon rate ratio regime; otherwise, the error exponent would depend quadratically on the total signal energy transmitted in low signal-to-noise photon rate ratio regime [9]. This is verified in Fig. 5, where the points marked by stars near the high signal-to-noise photon rate ratio regime correspond to optimum operating points for different optical energy per bit indicated in the horizontal axis. Also, shown in (20), the noise-to-failure ratio of $N_n/\ln(f)$ determines the minimum error probability bound for a limited amount of optical energy (per bit) N_s. This says that both the noise and the lightpath failure probability exponent contribute equally in determining the optimum operating point. Finally, the asymptotic minimum error probability bound (20) approaches zero when we increase the optical energy (per bit). This implies that we can eliminate the saturation effect in the super-high signal-to-noise photon rate ratio regime if we choose the number of lightpaths optimally.
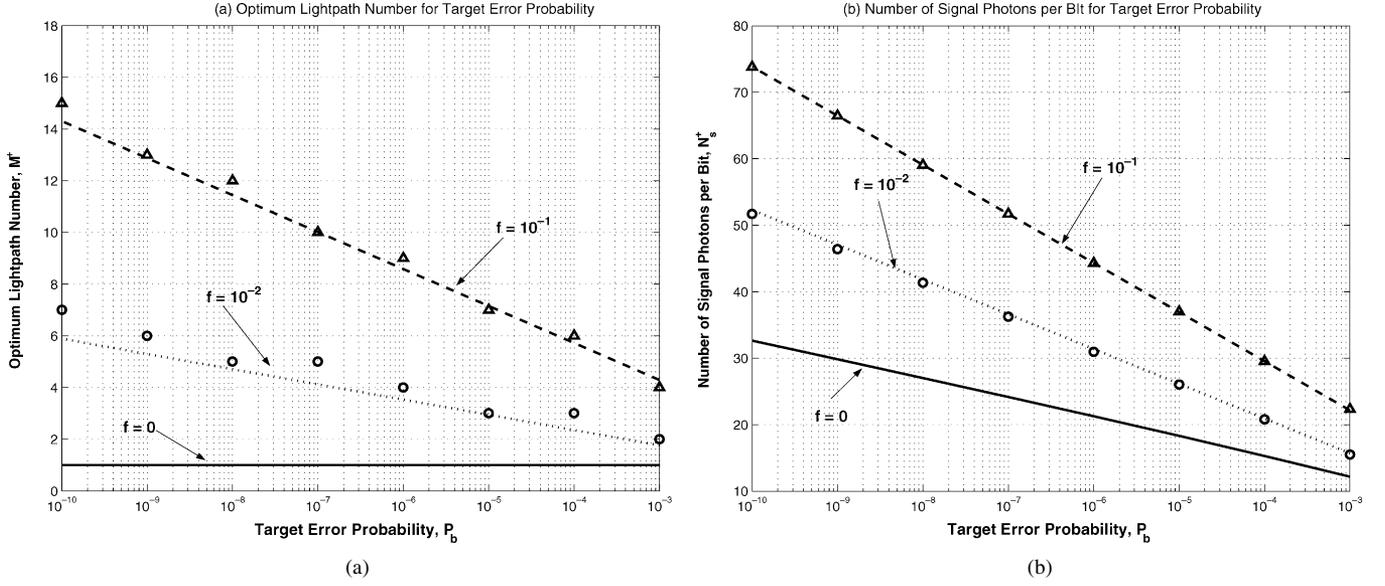
Fig. 7.   Number of lightpaths is chosen optimally to minimize the total energy per bit for target error probability bounds. (a) Shows the optimum number of lightpaths for various target error probability bounds. (b) Shows that the minimum optical energy per bit for various target error probability bounds. The lines are for analytical solutions, and the bullets for numerical solutions. We choose $N_n = 1$ for all the cases.

B. Minimizing the Total Optical Energy (Per Bit) N_s for a Target Error Probability Bound (PB_{GA})

In this section, we minimize the total transmitted optical energy (per bit) for a target error probability. Since the Chernoff bound (10) is exponentially tight, we can minimize the transmitted optical energy (per bit) for an equivalent target error probability bound. This is actually the dual of the problem investigated in Section IV-A.

For a given amount of optical energy (per bit) N_s, if we plug (17) into (19), we obtain the minimum error probability bound approximated by

$$P_b \approx \exp\left\{-N_s\Theta\left(f, N_n\right)\right\} \qquad (21)$$

where $\Theta\left(f, N_n\right) = -\ln\left(2f\right)/\zeta\left(f, N_n\right) > 0$. Using (21), we obtain the required minimum optical energy (per bit) for a target error probability bound P_b, given by

$$N_s^\dagger = \frac{-\ln\left(P_b\right)}{\Theta\left(f, N_n\right)}. \qquad (22)$$

Substituting (22) into (17), the optimal number of lightpaths to minimize the transmitted energy (per bit) is obtained as

$$M^\dagger = \frac{\ln\left(P_b\right)}{\ln\left(2f\right)} = \log_{2f}\left(P_b\right). \qquad (23)$$

In Fig. 7, we plot the optimum lightpath number $M^\dagger$ and the minimum optical energy (per bit) $N_s^\dagger$ versus different target error probability bounds according to the analytical solutions (22) and (23). As a comparison, the numerical results from an exhaustive search algorithm are also labeled as bullets points. Also, in Fig. 7, the case of $f = 0$ is plotted for reference. If the lightpath is perfectly reliable (i.e., $f = 0$), lightpath diversity is not used since using more lightpaths only increases the total noise and degrades the error performance as suggested by (12).

As shown in Fig. 7, both the optimal number of lightpaths and the minimum optical energy (per bit) increase with lower target error probabilities, because each lightpath is biased at the optimum operating point to have error probability of $2f$ by requiring an optimum average number of photons (per bit). We also note from Fig. 7 that more lightpaths are needed to achieve a target error probability bound when the reliability of individual lightpath deteriorates.

In (23), we cannot directly observe the effect of noise in determining the optimum lightpath number $M^\dagger$. As implied by (19), at the optimum operating point, each lightpath is biased to have error probability of $2f$, which is independent of the noise N_n. At the same time, in order to work at the optimum operating point, each lightpath requires an optimum average number of signal photons (per bit) given by (18). Therefore, when the noise increases, instead of requiring more lightpaths, we increase the total optical energy (per bit) to maintain the signal-to-noise photon rate ratio and, thus, bias each lightpath to have an effective error probability of $2f$. In fact, if we let $f \ll 1$, the required minimum optical energy (per bit) is approximated by

$$N_s^\dagger \approx -\ln\left(P_b\right)\left[1 + 2\sqrt{-\frac{N_n}{\ln\left(f\right)}}\right]. \qquad (24)$$

This says that, if we increase N_n, the required minimum optical energy (per bit) increases to bias each lightpath to have an effective error probability of $2f$ and, thus, the target error probability bound is achieved without requiring more lightpaths.

V. Optimum Realizable Receivers

Pragmatic engineering design is basically a tradeoff between implementation complexity and symbol error probability. In general, in order to achieve a lower error probability, the receiver needs to estimate states of all the lightpaths for symbol decisions. This joint estimation and detection approach can

result in a complicated receiver structure. On the other hand, a simpler receiver uses simpler lightpath state estimators or does not estimate the lightpath states at all and, thus, usually has a higher error probability. To highlight this tradeoff, we explore two extreme cases for the complexity-error tradeoff in this paper.

1) *Optimal receiver*: It has the lowest symbol error probability, but has the most complicated receiver architecture. This will be investigated in this section.

2) *EGC receiver*: The receiver architecture is much simpler. However, the error performance is suboptimum since it does not exploit all the available information at the receiver. This will be investigated in the next section.

Between the two extreme cases are other reasonably good suboptimal receivers. Their error performance is usually better than that of the EGC receiver, and worse than that of the optimal receiver. On the other hand, their complexity falls between the most complicated optimal receiver and the simplest EGC receiver. One of our objectives in this research is to see how these receivers perform in different signal-to-noise photon rate ratio regimes and generalize rules of thumb to balance the complexity-error tradeoff in practical optical receiver design.

In this section, we first find the optimal counting receiver under the following framework. At the optical signal processing module, optical delay lines are used to compensate for delay variations among different lightpaths (fiber delays can also be replaced by time delays in the electrical processing stage since we will use M parallel detectors); at the detection module, M photon-counting receivers are used to record the photo-event times for symbol decisions; at the electrical processing module, to minimize the symbol decision error probability, we use a ML detector to make symbol decisions based on the recorded photo-event time statistic.

A. Optimum Receiver Architecture

We start with the calculation of the likelihood functions for both hypotheses. For the ith channel, let (k_{i1}, k_{i2}) be photo-event counts during the first half bit interval $[0, T/2]$ and the second half bit interval $[T/2, T]$, and $(\underline{t}_{i1}, \underline{t}_{i2}) = (t_1, t_2, \ldots, t_{k_{i1}}, t_{k_{i1}+1}, t_{k_{i1}+2}, \ldots, t_{k_{i1}+k_{i2}})$ be the corresponding photo-event time statistic. The conditional distribution density functions of the time statistic at the ith lightpath output, as derived in [9], are given by

$$p(\underline{t}_{i1}, \underline{t}_{i2}|H_0)$$
$$= \left[\prod_{j=1}^{k_{i1}} \left(\widehat{F}_i^{(0)}(t_j) \frac{\lambda_s}{M} + \lambda_n \right) \right] (\lambda_n)^{k_{i2}} e^{-(\lambda_s/M) \int_0^{T/2} \widehat{F}_i^{(0)}(t) dt - 2N_n}$$

$$(25a)$$

and

$$p(\underline{t}_{i1}, \underline{t}_{i2}|H_1)$$
$$= (\lambda_n)^{k_{i1}} \left[\prod_{j=1}^{k_{i2}} \left(\widehat{F}_i^{(1)}(t_{j+k_{i1}}) \frac{\lambda_s}{M} + \lambda_n \right) \right] e^{-(\lambda_s/M) \int_{T/2}^T \widehat{F}_i^{(1)}(t) dt - 2N_n}$$

$$(25b)$$

where the minimum mean-squared error (MMSE) causal estimate of the ith lightpath state for hypotheses H_j ($j = 0, 1$) is given by

$$\widehat{F}_i^{(j)}(t) = \begin{cases} E\left[F_i^{(j)} | H_j, N_t = 0 \right], & N_t = 0 \\ E\left[F_i^{(j)} | H_j, N_t = k, \underline{t}_{i1}, \underline{t}_{i2} \right], & N_t = k \geq 1 \end{cases}$$

$$(26)$$

and N_t is the number of photo-events over $[0, t]$. As derived in Appendix C, these estimators are given by

$$\widehat{F}^{(0)}(t) = \frac{1}{1 + \frac{f}{1-f} \exp\left(\frac{\lambda_s}{M} t\right) (1 + \Omega)^{-N_t}} \quad t \in \left[0, \frac{T}{2}\right]$$

$$(27a)$$

where N_t is the number of photo-events over $[0, t]$, and

$$\widehat{F}^{(1)}(t) = \frac{1}{1 + \frac{f}{1-f} e^{(\lambda_s/M)(t-(T/2))} (1 + \Omega)^{-(N_t - N_{T/2})}}$$

$$t \in \left[\frac{T}{2}, T\right] \quad (27b)$$

where N_t is the photon count over $[0, t]$, and $N_{T/2}$ is the photon count over $[0, T/2]$ of the same realization of the photo-event process.

Note that the photo-event time statistics of the lightpaths are independent because the lightpaths belong to different shared-risk groups. It follows that the overall conditional distribution density functions can be written as

$$p(\underline{t}_1, \underline{t}_2|H_0) = \prod_{i=1}^M p(\underline{t}_{i1}, \underline{t}_{i2}|H_0) \quad (28a)$$

and

$$p(\underline{t}_1, \underline{t}_2|H_1) = \prod_{i=1}^M p(\underline{t}_{i1}, \underline{t}_{i2}|H_1) \quad (28b)$$

where $(\underline{t}_1, \underline{t}_2) = (\underline{t}_{11}, \underline{t}_{21}, \ldots, \underline{t}_{M1}, \underline{t}_{12}, \underline{t}_{22}, \ldots, \underline{t}_{M2})$ is the overall photo-event time statistics. Using (28a) and (28b), the log-likelihood ratio can be written as

$$\ln \Lambda \{\underline{t}, \underline{N}_1, \underline{N}_2 : 0 \leq t \leq T\}$$
$$= \ln \frac{p(\underline{t}_1, \underline{t}_2, \underline{N}_1, \underline{N}_2|H_0)}{p(\underline{t}_1, \underline{t}_2, \underline{N}_1, \underline{N}_2|H_1)}$$
$$= \sum_{i=1}^M \left[\sum_{j=1}^{k_{i1}} \ln\left(1 + \widehat{F}_i^{(0)}(t_j)\Omega\right) - \frac{\lambda_s}{M} \int_0^{T/2} \widehat{F}_i^{(0)}(t) dt \right]$$
$$- \sum_{i=1}^M \left[\sum_{j=1}^{k_{i2}} \ln\left(1 + \widehat{F}_i^{(1)}(t_{j+k_{i1}})\Omega\right) - \frac{\lambda_s}{M} \int_{T/2}^T \widehat{F}_i^{(1)}(t) dt \right]$$

$$(29)$$

where $\Omega = \lambda_s/M\lambda_n = N_s/MN_n$ is the signal-to-noise photon rate ratio. After some algebraic manipulations, we obtain the ML detection rule as

$$\sum_{i=1}^M \left\{ \sum_{j=1}^{k_{i1}} \ln\left(1 + \widehat{F}_i^{(0)}(t_j)\Omega\right) - \frac{\lambda_s}{M} \int_0^{T/2} \widehat{F}_i^{(0)}(t) dt \right\}$$
$$\underset{\widehat{H}=H_1}{\overset{\widehat{H}=H_0}{\underset{<}{\gtrless}}} \sum_{i=1}^M \left\{ \sum_{j=1}^{k_{i2}} \ln\left(1 + \widehat{F}_i^{(1)}(t_{j+k_{i1}})\Omega\right) - \frac{\lambda_s}{M} \int_{T/2}^T \widehat{F}_i^{(1)}(t) dt \right\}.$$

$$(30)$$
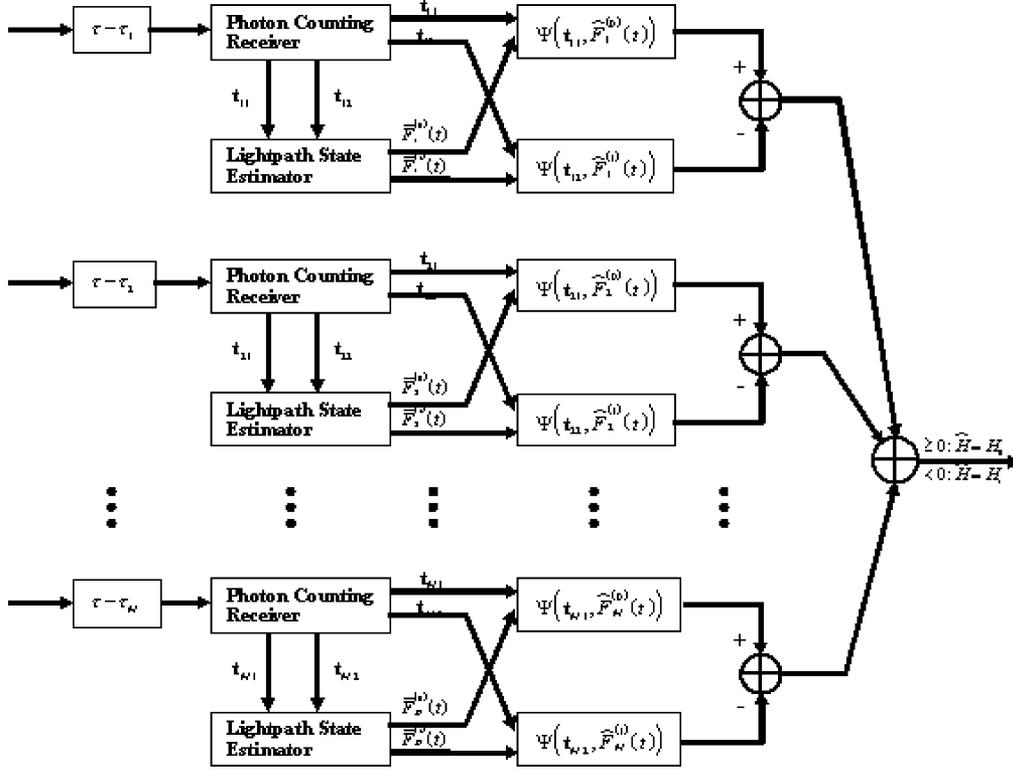
Fig. 8. Optimal receiver architecture. $\Psi_1\left(\mathbf{t}_{i1}, \widehat{F}_i^{(0)}(t)\right) = \sum_{j=1}^{k_{i1}} \ln\left(1 + \widehat{F}_i^{(0)}(t_j)\,\Omega\right) - \frac{\lambda_s}{M}\int_0^{T/2} \widehat{F}_i^{(0)}(t)dt$, where $\mathbf{t}_{i1}$ are photo-event time statistics and $\widehat{F}_i^{(0)}(t)$ are channel state estimators under H_0. $\Psi_2\left(\mathbf{t}_{i2}, \widehat{F}_i^{(1)}(t)\right) = \sum_{j=1}^{k_{i2}} \ln\left(1 + \widehat{F}_i^{(1)}(t_{j+k_{i1}})\,\Omega\right) - \frac{\lambda_s}{M}\int_{T/2}^T \widehat{F}_i^{(1)}(t)\,dt$, where $\mathbf{t}_{i2}$ are photo-event time statistics and $\widehat{F}_i^{(1)}(t)$ are channel state estimators under H_1.

For a sanity check, assume all the lightpaths are UP, i.e., $\widehat{F}_i^{(0)}(t) = \widehat{F}_i^{(1)}(t) = 1$, during the symbol transmission, the decision rule (30) turns out to be

$$\sum_{i=1}^M k_{i1} \underset{\widehat{H}=H_1}{\overset{\widehat{H}=H_0}{\underset{<}{\gtrless}}} \sum_{i=1}^M k_{i2}. \tag{31}$$

Note that the detection rule (31) is identical to the detection rule for the case with invulnerable lightpaths [12].

Note that each received photon is weighed by the scaling factor $\ln\left(1 + \widehat{F}(t_j)\,\Omega\right)$ which depends on the lightpath state estimate at the photon arrival time. If the estimate of the lightpath state is large meaning that the possibility of the lightpath being UP is high, the scaling factor is large since it is more likely that the photon comes from the signal, not the noise. On the contrary, we assign a small scaling factor to the photon if the lightpath state estimate is small. In particular, if we estimate that the lightpath is DOWN, the scaling factor is equal to zero since the photon must come from noise and, thus, should not be taken into consideration for detection.

Moreover, detection rule (30) indicates a fundamental decomposition of functions in the optimal receiver structure, which is generalized as the separation theorem of detection in [9]. In particular, the receiver consists of two separable operation modules, i.e., estimators for lightpath states and signal processing modules for hypothesis testing, as shown in Fig. 8. This sep-

aration property suggests that we may be able to replace the complicated optimal lightpath state estimator with some simpler heuristic state estimators to reduce the receiver complexity without modifying the receiver structure. This idea often performs well in practice and yields near-optimal policies in dynamic programming [18]. Therefore, we expect that the error performance with suboptimal lightpath state estimators is not degraded significantly, which indeed is true, as will be shown in next section.

B. Error Performance

In this section, we analyze the error performance of the optimal receiver. In particular, a lower bound and an upper bound are derived for the exponentially tight Chernoff bound of the symbol error probability.

As illustrated in Section III, the symbol error probability of the "genie-aided" receiver is the "genie-aided" limit of the proposed architecture within the class of structured receivers. For a sense of how well the optimal receiver performs, we can use the Chernoff bound of the "genie-aided" receiver as a lower bound for Chernoff bound of the optimal receiver because the Chernoff bound is exponentially tight [12]. This suggests that the following lower bound for the Chernoff error bound of the optimal receiver

$$\mathrm{PB}_{\mathrm{opt}} \geq \left[f + (1-f)\,e^{-\psi(N_s, N_n, M)}\right]^M \triangleq \mathrm{PB}_{\mathrm{opt}}^{LB} \tag{32}$$

where $\psi\left(N_s, N_n, M\right) = \left(\sqrt{N_s/M + N_n} - \sqrt{N_n}\right)^2$, $N_s = \lambda_s T/2$ is the average number of signal-driven photo-events per bit, $N_n = \lambda_n T/2$ is the average number of noise-driven photo-events per 1/2 bit, and $\mathrm{PB}_{\mathrm{opt}}$ is the error bound of the optimal receiver.

On the other hand, the optimal receiver must perform better than any suboptimal receiver within the class of structured receivers [11]. It follows that we can use the Chernoff bound of any suboptimal receiver as an upper bound for the performance of the optimal receiver. In particular, we choose a suboptimal receiver that uses the following noncausal estimator

$$\begin{aligned} \text{if } \widehat{F}(T) &\leq 0.5, \qquad \widetilde{F} = 0 \\ \text{if } \widehat{F}(T) &> 0.5, \qquad \widetilde{F} = 1 \end{aligned} \qquad (33)$$

where $\widehat{F}(T)$ is the MMSE causal estimate of the channel state at time $t = T$ and $\widetilde{F}$ is the estimated lightpath state. If $\widetilde{F} = 0$, the receiver estimates the lightpath to be DOWN and, thus, discards the received signal over that lightpath. Otherwise, the receiver estimates the lightpath to be UP and, thus, uses the received optical signal over that lightpath for optimal combining and symbol decisions.

As derived in Appendix D, the upper bound for the Chernoff error bound of the optimal receiver, which is also the Chernoff error bound of the suboptimal receiver, is given by

$$\mathrm{PB}_{\mathrm{opt}} \leq \left[g + (1 - g)\, e^{-\psi(N_s, N_n, M)}\right]^M \triangleq \mathrm{PB}_{\mathrm{opt}}^{\mathrm{UP}}. \qquad (34)$$

Here, the probability that the lightpath is estimated to be DOWN, $g = \Pr\left(\widehat{F}(T) \leq 1/2\right)$, is given by

$$\begin{aligned} g = f \sum_{k=0}^{N_{TH}} \frac{\left(N_n\right)^k}{k!} e^{-N_n} \\ + (1 - f) \sum_{k=0}^{N_{TH}} \frac{\left(\frac{N_s}{M} + N_n\right)^k}{k!} e^{-((N_s/M) + N_n)}. \end{aligned} \qquad (35)$$

where

$$N_{TH} = \frac{\frac{N_s}{M} + \ln\left(\frac{f}{(1-f)}\right)}{\ln\left(1 + \frac{N_s}{MN_n}\right)} \qquad (36)$$

is the number of photons per bit beyond which the lightpath is estimated to be UP. In (36), N_s/M is the average number of photons per lightpath per bit, $\ln\left[f/(1-f)\right]$ is the additional number of photons needed to declare that the lightpath is UP, and both numbers must be adjusted by the term $\ln\left(1 + N_s/MN_n\right)$, which is the scaling factor in (30), to obtain the actual number of photons. If $0 < f < 1/2$, then $\ln\left[f/(1-f)\right] < 0$. This means that the actual number of photons needed is reduced since the probability of the lightpath being UP is higher and fewer photons per lightpath are needed for the estimator to declare that the lightpath is UP. On the other hand, if $1/2 < f < 1$, then $\ln\left[f/(1-f)\right] > 0$. This means that the actual number of photons needed is increased since the probability of the lightpath being DOWN is higher and more photons per lightpath are needed for the estimator to declare that the lightpath is UP.
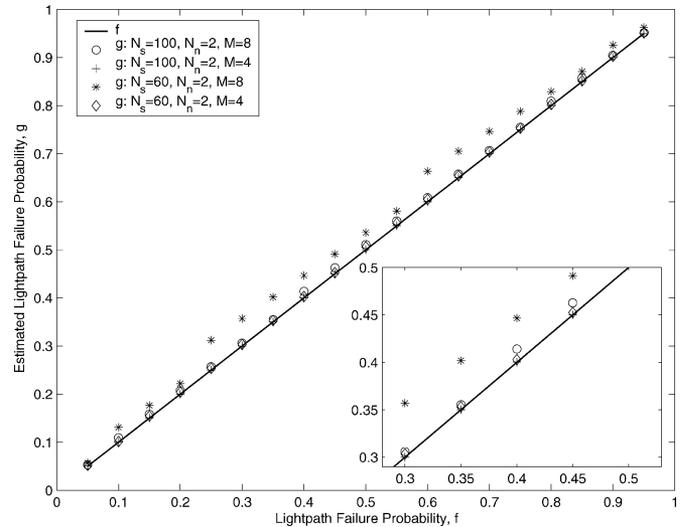
Fig. 9. Estimated lightpath failure probability g is compared with the prior lightpath failure probability f under different signal-to-noise photon rate ratios.
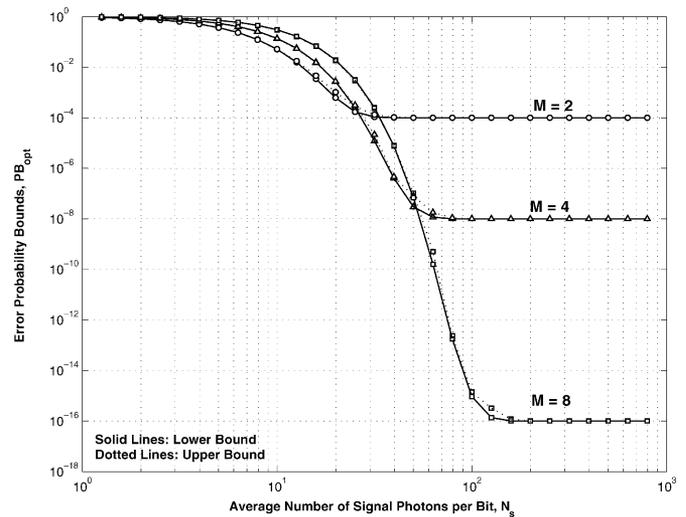
Fig. 10. Lower bound and the upper bound for the Chernoff bound of the optimal receiver. ($f = 0.01$ and $N_n = 2$).

Note that the lower bound (32) and the upper bound (34) have the same form, except that the prior lightpath failure probability f in (32) is replaced by the estimated lightpath failure probability g in (34). This implies that the tightness of the lower bound and the upper bound highly depends on the difference between the estimated lightpath failure probability and the prior lightpath failure probability. To explore this, we compare the estimated lightpath failure probability g with the prior failure probability f in Fig. 9. We find that the difference between these two probabilities is negligible when the signal-to-noise photon rate ratio is high enough. It follows that the lower bound and the upper bound are close to each other and, thus, both are very tight. This is verified in Fig. 10, where the lower bound and the upper bound are plotted against the average number of signal photons per bit. Moreover, these tight bounds suggest that the optimal receiver exhibits the

same error characteristics in different signal-to-noise photon rate ratio regimes as the "genie-aided" receiver, as shown in Fig. 10. In the super-high signal-to-noise photon rate ratio regime, the error bound converges to an error floor f^M, the probability with which the source–destination pair is disconnected. This suggests that network topologies with small probability of disconnection [6], [7] should be considered for ultrahigh reliable optical networks. In the lower signal-to-noise photon rate ratio regime, the error probability increases with more lightpaths. It indicates that lightpath diversity actually hurts in this regime and be of no engineering interest. In the medium-to-high signal-to-noise photon rate ratio regime, the error probability depends on both the number of lightpaths and the signal-to-noise photon rate ratio. These two factors, however, are competing with each other for a given amount of optical energy. Hence, we need to balance this tradeoff to achieve better energy efficiency. This, along with the fact that the optimal receiver performs close to the "genie-aided" receiver limit, suggests that system parameters optimized for the "genie-aided" receiver, such as the optimum number of lightpaths derived for different objective functions, also apply for the optimal receiver in the medium-to-high signal-to-noise photon rate ratio regime.

VI. EQUAL-GAIN-COMBINING (EGC) RECEIVER

Although the optimal receiver has the lowest symbol error probability, it involves complicated processing by estimating the individual lightpath state throughout the symbol duration. In this section, we develop one suboptimal receiver, the EGC receiver, which not only approaches the optimal receiver in the symbol error probability under most scenarios, but also has the advantage of a simpler architecture.

A. Receiver Architecture

In the EGC receiver, rather than estimating lightpath states, we assume all the lightpaths to be UP and use the ML decision rule to do symbol detection. Mathematically, the EGC receiver employs the following decision rule:

$$\sum_{i=1}^{M} k_{i1} \underset{\widehat{H}=H_1}{\overset{\widehat{H}=H_0}{\underset{<}{\gtrless}}} \sum_{i=1}^{M} k_{i2} \qquad (37)$$

to make symbol-to-symbol decision based only on the photo-event counts. Decision rule (37) is much simpler than decision rule (30) in that only one photon-counting receiver is needed. This indicates that the EGC receiver offer a significant reduction in implementation complexity compared with the optimal receiver, at the expense of a degraded error performance, as shown in the following section.

B. Error Performance

We start with the calculation of the error bound for the EGC receiver. Given the lightpath state vector $\mathbf{F}$, the conditional error probability is defined by

$$\Pr(\varepsilon|\mathbf{F}) = p_0 \Pr\left[\sum_{i=1}^{M} k_{i1} \leq \sum_{i=1}^{M} k_{i2} | H_0, \mathbf{F}\right]$$
$$+ p_1 \Pr\left[\sum_{i=1}^{M} k_{i1} \geq \sum_{i=1}^{M} k_{i2} | H_1, \mathbf{F}\right]$$
$$= \Pr\left[\sum_{i=1}^{M} k_{i1} \leq \sum_{i=1}^{M} k_{i2} | H_0, \mathbf{F}\right] \qquad (38)$$

where p_0, p_1 are probabilities of sending the "ZERO" or "ONE" bit, and the second equality is due to the symmetry of binary pulse-position modulation and $p_0 = p_1 = 1/2$ for equiprobable digital source.

Let $K_1 = \sum_{i=1}^{M} k_{i1}$ be the total photo-event count recorded over $[0, T/2]$, and $K_2 = \sum_{i=1}^{M} k_{i2}$ be the total photo-event count recorded over $[T/2, T]$. Note that, given hypothesis H_0 and the lightpath state vector $\mathbf{F}$, K_1 is a Poisson random variable with mean $mN_s/M + MN_n$, where $m = \sum_{i=1}^{M} F_i$ is the number of UP lightpaths for a given lightpath state vector $\mathbf{F}$, and K_2 is a Poisson random variable with mean MN_n.

Using the Chernoff bound, the conditional error probability is bounded by

$$\Pr(\varepsilon|\mathbf{F}) \leq \exp\left\{ -\left(\sqrt{m\left(\frac{N_s}{M}\right) + MN_n} - \sqrt{MN_n}\right)^2\right\}. \qquad (39)$$

It can be verified that m is a binominal random variable with a distribution function of $\Pr\{m = k\} = \binom{M}{k}(1-f)^k f^{M-k}$, $k = 0, 1, \ldots, M$. Averaging (20) over all possible lightpath state vectors $\mathbf{F} \in \{0, 1\}^M$, we obtain the error bound for the EGC receiver, as shown in (40) at the bottom of the page.

Using (40), we compare the error bound of the EGC receiver with the "genie-aided" receiver limit in Fig. 11. In the low signal-to-noise photon rate ratio regime, the error probability is inherently high and of no engineering interest. In the medium-to-high signal-to-noise photon rate ratio regime, the gap between error bounds of the EGC receiver and the "genie-aided" limit is larger than the gap between error bounds of the optimal receiver and the "genie-aided" limit. With the EGC receiver, noise from DOWN lightpaths will degrade the average signal-to-noise photon rate ratio and, thus, increases the error probability since the error probability in the medium-to-high signal-to-noise photon rate ratio regime is

$$\Pr(\varepsilon) \leq \sum_{k=0}^{M} \frac{M!}{k!\,(M-k)!} (1-f)^k f^{M-k} e^{-\left(\sqrt{N_s(k/M)+MN_n} - \sqrt{MN_n}\right)^2} \qquad (40)$$
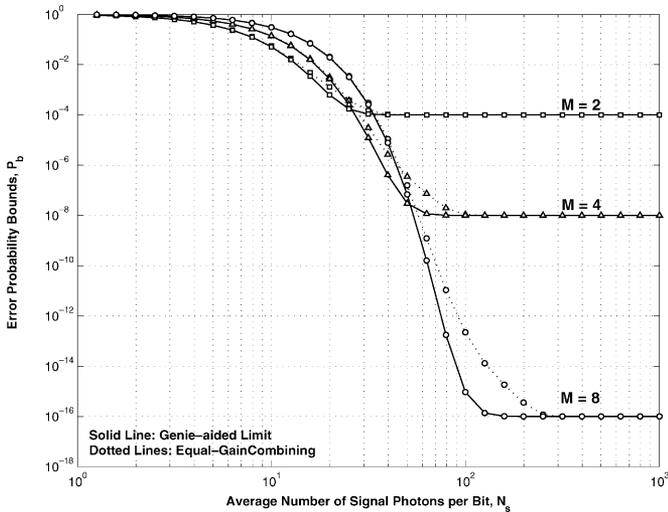
Fig. 11. Error bounds of the EGC receiver are compared with the "genie-aided" receiver limit under different lightpath numbers. ($f = 0.01$ and $N_n = 2$).

sensitive to the signal-to-noise photon rate ratio. However, in the high signal-to-noise photon rate ratio regime, the EGC receiver has an error bound close to the "genie-aided" receiver limit. This indicates that the EGC receiver is preferable to the optimal receiver in the high signal-to-noise photon rate ratio regime due to its simplicity. In fact, the EGC receiver approaches asymptotically the optimal receiver when the noise is negligible, as we will show next.

C. Power Penalty

Since the error probability of the EGC receiver is higher than that of the "genie-aided" receiver, we need to transmit more optical energy in order for the EGC receiver to achieve the same target error probability as the "genie-aided" receiver does in the medium-to-high signal-to-noise photon rate ratio regime. In this section, we analyze this amount of additional power for the EGC receiver to achieve a target error probability bound compared with the "genie-aided" receiver. For a target error probability bound of P_b, the power penalty of the EGC receiver over the "genie-aided" receiver is defined as

$$\delta = 10 \log_{10} \left(\frac{N_s^* (P_b, f, N_n; \text{EGC})}{N_s^* (P_b, f, N_n; \text{GA})} \right) \qquad (41)$$

where $N_s^* (P_b, f, N_n; \text{GA})$ and $N_s^* (P_b, f, N_n; \text{EGC})$ are the minimum amounts of optical power (in terms of average number of signal photons per bit) for the "genie-aided" receiver and the EGC receiver, respectively, to achieve a target error probability P_b.

Using numerical results by exhaustive searching, the optimal number of lightpaths and the minimum transmitted optical energy are plotted in Fig. 12(a) and (b). To achieve the same error probability bound, the EGC receiver requires more lightpaths and more optical energy. This suggests that a more densely connected network topology is needed to provide enough independent lightpaths for the EGC receiver. The power penalty is plotted in Fig. 12(c) and (d). From Fig. 12(c), the power penalty

is asymptotically independent of the target error probability. This is due to two reasons. First, the error bound of the EGC receiver is close to that of the "genie-aided" receiver with optimized system parameters. Second, the minimum transmitted power is linear with the error exponent given by (22) in Section IV-B. It follows that, at the optimum operating points, both error bounds are parallel to each other in a log-log plot. The power penalty is approximately determined by the ratio between the slopes of the error exponents of the "genie-aided" receiver and the EGC receiver at the respective optimum operating points. Therefore, the power penalty is independent of the target error probability bounds. On the other hand, the power penalty increases with higher noise levels as shown in plot (d), and approaches zero when the noise level goes to zero. This demonstrates that the EGC receiver is generally suboptimal and approaches the optimal receiver when the noise level decreases. In particular, if there is no noise, the EGC receiver would be optimal because the receiver would not receive any noise from DOWN lightpaths to degrade the error performance. Moreover, for the practically interesting parameters, the power penalty is around 1-dB. In practical system design, if this 1-dB penalty is acceptable, the equal-gain-combing receiver is preferable over the optimum receiver due to its simplicity.

VII. CONCLUSION

In this paper, we proposed the use of lightpath-diversity to achieve ultra-reliable end-to-end communication with low delay requirements in all-optical networks. For a network with dense connections, arbitrary reliability can be achieved if enough independent lightpaths are used. Since this approach is implemented entirely at the Physical Layer without the use of higher layer protocols such as ARQs, the response is fast enough for applications with super-high date rates and/or critical time deadlines.

From a theoretical perspective, we have characterized the proposed lightpath-diversity system with a Doubly Stochastic Point Process model. The limit on the error probability of the scheme has been obtained via a "genie-aided" receiver. This "genie-aided" receiver limit serves as a benchmark for practical receiver architectures. Under typical operating scenarios, we have optimized the system performance by choosing an optimal number of lightpaths to utilize the limited optical power efficiently. Analytical proof showed that each lightpath requires an optimum number of signal photons to bias itself at the effective error probability of $2f$. This optimum average number of photons per lightpath is fully determined by the lightpath parameters, including the lightpath failure probability and the noise level.

From an engineering perspective, we have investigated the class of structured receivers for the multiple-lightpath transmission architecture. Using the Doubly Stochastic Point Process model, we have developed the architecture of the optimal receiver, and have bounded its error performance with a lower bound (the "genie-aided" receiver) and an upper bound (non-causal estimator). The tightness of the lower bound and the upper bound indicates that the optimal receiver approaches the "genie-aided" limit of structured receivers and, thus, system parameters optimized for the "genie-aided" receiver apply to the optimal receiver in the medium-to-high signal-to-noise photon
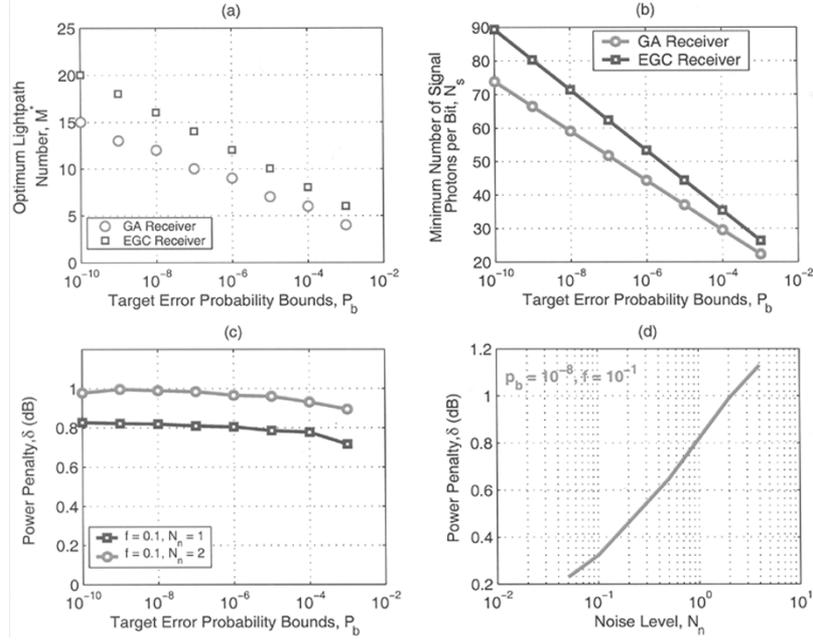
Fig. 12. (a) Optimal lightpath number to minimize the total optical energy is plotted against different target error probability bounds. (b) The minimum number of signal photons per bit is plotted against different target error probability bounds for the "genie-aided" receiver and the EGC receiver. In (a) and (b), we set $f = 0.1$ and $N_n = 2$. GA: genie-aided receiver; EGC: equal-gain-combining receiver. (c) Power penalty of the EGC receiver is plotted under different target error probability bounds. (d) Power penalty of the EGC receiver is plotted under different noise levels.

photon rate ratio regime. However, the optimal receiver needs to estimate lightpath states throughout the symbol time, which is complicated. To balance error probability performance and implementation complexity, we have developed a suboptimal EGC receiver with lower complexity, and have characterized its error performance. Performance comparison between the equal-gain-combining receiver and the "genie-aided" receiver limit of structured receiver showed that the power penalty of the EGC receiver decreases with decreasing noise level. These results suggest that the equal-gain-combining receiver is preferable to the optimal receiver in the high signal-to-noise photon rate ratio regime, and the optimal receiver is needed for good performance in the low signal-to-noise photon rate ratio regime at the expense of increased complexity. For practical system design, if the marginal 1-dB penalty is acceptable, the equal-gain-combining receiver is always the preferable due to its simplicity.

APPENDIX A
OPTIMUM POWER ALLOCATION ALGORITHM FOR HOMOGENOUS LIGHTPATHS

For a M-connected source-destination pair, the power allocation vector is $\mathbf{P} = (P_1, P_2, \ldots, P_M)^T \in \mathbb{R}^+$, and the state vector is $\mathbf{F} = (F_1, F_2, \ldots, F_M)^T$ with a probability distribution $\Pr(\mathbf{F}) = f^{\sum_{i=1}^{M} F_i}(1-f)^{M-\sum_{i=1}^{M} F_i}$. For the "genie-aided" receiver, the overall error probability upper bound is given by

$$\mathrm{PB}_{\mathrm{GA}} = \sum_{\mathbf{F} \in \{0,1\}^M} \Pr(\mathbf{F}) e^{-\left(\sqrt{\mathbf{F}^T(\mathbf{P}+\mathbf{N}_n)} - \sqrt{\mathbf{F}^T\mathbf{N}_n}\right)^2} \quad (A.1)$$

where $\mathbf{N}_n = (N_n, N_n, \ldots, N_n)^T$ is the noise power vector and $\{0,1\}^M$ is the M-dimensional vector space over the $\{0,1\}$ field.

To minimize the error probability, we solve the following nonlinear programming problem

$$\min h(\mathbf{P}) = \sum_{\mathbf{F} \in \{0,1\}^M} \Pr(\mathbf{F}) e^{-\left(\sqrt{\mathbf{F}^T(\mathbf{P}+\mathbf{N}_n)} - \sqrt{\mathbf{F}^T\mathbf{N}_n}\right)^2}$$
$$s.t. \ \mathbf{P}^T\mathbf{1} = P_s \quad (A.2)$$

where $\mathbf{1} = (1, 1, \ldots, 1)^T$.

From the fact that, for each $\mathbf{F} = (F_1, F_2, \ldots, F_M) \in \{0,1\}^M$, the function $\exp\left\{-\left(\sqrt{\mathbf{F}^T(\mathbf{P}+\mathbf{N}_n)} - \sqrt{\mathbf{F}^T\mathbf{N}_n}\right)^2\right\}$ is a convex function defined over a compact convex set $\left\{(P_1, P_2, \ldots, P_M) \in \mathbb{R}^+ : \sum_{i=1}^{M} P_i = P_s\right\}$, we conclude that the objective function $h(\mathbf{P})$ is convex over the compact convex set. It follows that the minimization problem (A.2) has a unique solution due to the convex property.

From the Karush–Kuhn–Tuck conditions [14], we have

$$\nabla_{\mathbf{P}} L(\mathbf{P}, \mu) = 0 \quad (A.3)$$

where $L(\mathbf{P}, \mu) = h(\mathbf{P}) - \mu(\mathbf{P}^T\mathbf{1} - P_s)$, and μ is a Lagrange multiplier. It can be verified that the following power allocation vector

$$\mathbf{P} = \left(\frac{P_s}{M}, \frac{P_s}{M}, \ldots, \frac{P_s}{M}\right)^T \quad (A.4)$$

satisfies the necessary condition of (A.3). It follows that (A.4) must be the unique minimizer of the objective function. This result indicates that the uniform power allocation algorithm is optimal under the assumption of homogenous lightpaths.

APPENDIX B
OPTIMUM NUMBER OF LIGHTPATHS USED FOR A LIMITED AMOUNT OF TRANSMITTED OPTICAL ENERGY

In this section, we solve the nonlinear programming problem given by

$$\min_{M>0} G(M) = (f + (1-f)\exp\{-\psi(N_s, N_n, M)\})^M. \tag{B.1}$$

From the implicit function theorem [14], there exists a function $M^* = \varphi(N_s, N_n, f)$ such that $G(M)$ is minimized over the convex set $\{M : M \in \mathbb{R}^+\}$. We find an approximation of the function $M^* = \varphi(N_s, N_n, f)$ as follows.

Let $a = f$ and $b(M) = (1-f)\exp\{-\psi(N_s, N_n, M)\}$. Note that $0 \le a, b(M) \le 1$ and $G(M) = (a + b(M))^M$. To a first-order approximation, in the medium signal-to-noise photon rate ratio regime, the optimum number M^* of lightpaths can be approximated by the value of M, where the curve a^M and the curve b^M meet, i.e.,

$$a^M = b(M)^M. \tag{B.2}$$

If $0 < f < 0.5$, (B.2) has a unique solution given by

$$M^* = \frac{N_s}{\ln\left(\frac{1}{f} - 1\right) + 2\sqrt{N_n}\sqrt{\ln\left(\frac{1}{f} - 1\right)}}. \tag{B.3}$$

This approximation is found to be very accurate when compared with a numerical search for M^*.

Intuitively, this derivation can be understood as follows. For each individual lightpath channel, there are two detrimental factors that degrade the error performance. One is the noise, the other is the lightpath failure. If the lightpath works in high signal-to-noise photon rate ratio regime, the error due to the noise is dominated by the error due to the lightpath failure such that the error probability is floored by the failure probability f. The energy efficiency in this regime is very low but error probability is also low. On the other hand, if the lightpath works in low signal-to-noise photon rate ratio regime, the error due to the noise dominates the error due to the lightpath failure such that the error probability is on the order of one. In this regime, the energy efficiency is high but the error probability is also high. As a tradeoff between the energy efficiency and the error probability, the optimal operation point should be the point where both noise and failure contribute equally to the error probability, i.e., $f = (1-f)\exp(-\psi(N_s, N_n, M))$. The optimal number of signal photons per lightpath follows from this observation.

APPENDIX C
MMSE LIGHTPATH STATE ESTIMATOR FOR OPTIMUM RECEIVER

In designing the optimal receiver, we need to find the MMSE causal estimator of lightpath states. We start by incorporating the following lemma in [9], which is crucial to the derivation of the MMSE causal lightpath state estimator.

Lemma 1 (Estimation of Random Variables in Doubly Stochastic Point Processes): For a doubly stochastic point-process $\{N(t) : t \ge t_0\}$ with a random arrival rate $\lambda(t, \mathbf{x})$, where $\mathbf{x}$ is a time-independent random vector, let $\mathbf{a}_t(\mathbf{x})$ be a time-dependent vector-value function of the random vector $\mathbf{x}$ and such that $E\left(|\mathbf{a}_t(\mathbf{x})|^2\right) < \infty$. Then, for a recorded time statistic $\{\mathbf{t} = (t_1, t_2, \ldots, t_n)\}$, the MMSE causal estimate of the function $\mathbf{a}_t(\mathbf{x})$ of $\mathbf{x}$ is the conditional mean $\widehat{\mathbf{a}}_t$, given by

$$\widehat{\mathbf{a}}_t = E[\mathbf{a}_t(\mathbf{x})|\mathbf{t} = (t_1, t_2, \ldots, t_n)] = \frac{E\{\mathbf{a}_t(\mathbf{x})\exp[\mathbf{A}_t(\mathbf{x})]\}}{E\{\exp[\mathbf{A}_t(\mathbf{x})]\}} \tag{C.1}$$

where $\mathbf{A}_t(\mathbf{x}) = -\int_{t_0}^t \lambda(\tau, \mathbf{x})d\tau + \int_{t_0}^t \ln\lambda(\tau, \mathbf{x})dN_\tau$. $\square$

For simplicity, the subscript i is suppressed in the following derivation. Due to the random channel model, the arrival rate of the photo-event process at the output of each detector $\lambda(t, F) = F\lambda(t) + \lambda_n$ is a random variable. In particular, F is a Bernoulli random variable with the probability density function $p_F(x) = f\delta(x) + (1-f)\delta(x-1)$.

Using (C.1), the MMSE causal estimator of the channel state F is given by

$$\widehat{F}(t) = E[F|\mathbf{t}] = \frac{E\{F\exp[A_t(F)]\}}{E\{\exp[A_t(F)]\}} \tag{C.2}$$

where $A_t(F) = -\int_0^t \lambda(\tau, F)d\tau + \int_0^t \ln\lambda(\tau, F)dN_\tau$.

For hypothesis H_0, the photo-event rate is

$$\lambda^{(0)}(t) = \begin{cases} \frac{F\lambda_s}{M} + \lambda_n, & 0 \le t \le \frac{T}{2} \\ \lambda_n, & \frac{T}{2} \le t \le T \end{cases}. \tag{C.3}$$

Substituting (C.3) into (C.2), the MMSE causal estimator of the channel state F turns out to be

$$\widehat{F}^{(0)}(t) = \frac{1}{1 + \frac{f}{1-f}\exp\left(\frac{\lambda_s}{M}t\right)(1+\Omega)^{-N_t}} \quad t \in \left[0, \frac{T}{2}\right]. \tag{C.4}$$

where N_t is the number of photo-events over $[0, t]$.

For hypothesis H_1, the photo-event rate is

$$\lambda^{(1)}(t) = \begin{cases} \lambda_n, & 0 \le t \le \frac{T}{2} \\ \frac{F\lambda_s}{M} + \lambda_n, & \frac{T}{2} \le t \le T \end{cases}. \tag{C.5}$$

Substituting (C.5) into (C.2), the MMSE causal estimator of the channel state F turns out to be

$$\widehat{F}^{(1)}(t) = \frac{1}{1 + \frac{f}{1-f}e^{(\lambda_s/M)(t-(T/2))}(1+\Omega)^{-(N_t - N_{T/2})}}$$
$$t \in \left[\frac{T}{2}, T\right]. \tag{C.6}$$

where N_t is the photo-event count over $[0, t]$, and $N_{T/2}$ is the number photo-event count over $[0, T/2]$ of the same sample function of photo-event process.

APPENDIX D
CHERNOFF BOUND OF THE SYMBOL ERROR PROBABILITY FOR THE RECEIVER WITH NONCAUSAL LIGHTPATH STATE ESTIMATOR

The suboptimal receiver makes hard-decisions on estimated lightpath states from causal state estimators at time $t = T$. The noncausal hard-decision rule is given by

$$\text{when } \widehat{F}(T) \le 0.5 \quad \widetilde{F} = 0$$
$$\text{when } \widehat{F}(T) > 0.5 \quad \widetilde{F} = 1 \tag{D.1}$$

where $\widehat{F}(T)$ is the MMSE causal estimate of the lightpath state at time $t = T$. If $\widetilde{F} = 0$, the receiver estimates the lightpath to be DOWN and, thus, discards the received signal over that lightpath. Otherwise, the receiver estimates the lightpath to be UP and, thus, uses the received optical signal over that lightpath for optimal combining and symbol decisions.

With hard-decision lightpath states, the symbol decision rule is given by

$$\sum_{i=1}^{m} k_{i1} \overset{\widehat{H}=H_0}{\underset{\widehat{H}=H_1}{\gtrless}} \sum_{i=1}^{m} k_{i2} \qquad \text{(D.2)}$$

where m is the number of lightpaths that are estimated to be UP during the symbol transmission. Note that m is a binomial random variable with a probability distribution function

$$\Pr(m) = \binom{M}{m} (1-g)^m \, g^{M-m} \qquad \text{(D.3)}$$

where $g = \Pr\left(\widehat{F}(T) \le 0.5\right)$ is the probability with which the lightpath is estimated to be DOWN during the symbol transmission. For both hypotheses, the channel state estimator has the form

$$\widehat{F} = \left[1 + \frac{f}{1-f} \exp\left(\frac{N_s}{M}\right)(1+\Omega)^{-N}\right]^{-1}. \qquad \text{(D.4)}$$

The probability distribution function of the photon count is

$$\Pr(N = k) = f \frac{(N_n)^k}{k!} e^{-N_n}$$
$$+ (1-f) \frac{\left(\frac{N_s}{M} + N_n\right)^k}{k!} e^{-((N_s/M)+N_n)}. \qquad \text{(D.5)}$$

Combining (D.4) and (D.5), the probability with which the lightpath is estimated to be DOWN is given by

$$g = \Pr\left(\widehat{F} \le 0.5\right)$$
$$= \Pr\left(N \le \frac{\frac{N_s}{M} + \ln(f) - \ln(1-f)}{\ln(1+\Omega)} \triangleq N_{TH}\right)$$
$$= \sum_{k=0}^{N_{TH}} \Pr(N = k). \qquad \text{(D.6)}$$

To calculate the error bound, we start with the error probability conditioned on the number of lightpaths estimated to be UP during the symbol time. For given m, the conditional error probability is defined as

$$\Pr(\varepsilon|m) = p_0 \Pr\left[\sum_{i=1}^{m} k_{i1} \le \sum_{i=1}^{m} k_{i2} \Big| H_0, m\right]$$
$$+ p_1 \Pr\left[\sum_{i=1}^{m} k_{i1} \ge \sum_{i=1}^{m} k_{i2} \Big| H_1, m\right]$$
$$= \Pr\left[\sum_{i=1}^{m} k_{i1} \le \sum_{i=1}^{m} k_{i2} \Big| H_0, m\right] \qquad \text{(D.7)}$$

where the second equality is due to the symmetry of BPPM. Using the Chernoff bound, the right-hand side of (D.7) is bounded by

$$\Pr\left[\sum_{i=1}^{m} k_{i1} \le \sum_{i=1}^{m} k_{i2} \Big| H_0, m\right]$$
$$\le \min_{s>0}\left\{e^{mN_n(e^s-1)} e^{m(N_s/M+N_n)(e^{-s}-1)}\right\}$$
$$= \exp\{-m\psi(N_s, N_n, M)\} \qquad \text{(D.8)}$$

where $\psi(N_s, N_n, M) = \left(\sqrt{N_s/M + N_n} - \sqrt{N_n}\right)^2$.

Using (D.6) and (D.8), the error bound of the hard-decision receiver is obtained by averaging (D.8) over all possible m, that is

$$\Pr(\varepsilon) = \sum_{m=0}^{M} \Pr(\varepsilon|m) \Pr(m)$$
$$\le \sum_{m=0}^{M} e^{-m\psi(N_s, N_n, M)} \binom{M}{m} (1-g)^m \, g^{M-m}$$
$$= \left[g + (1-g) e^{-\psi(N_s, N_n, M)}\right]^M. \qquad \text{(D.9)}$$

Note that (D.9) is also an upper bound for the optimal receiver.

REFERENCES

[1] V. W. S. Chan *et al.*, "A precompetitive consortium on wide-band all-optical networks," *IEEE/LEOS J. Lightw. Technol.*, vol. 11, no. 5/6, pp. 714–735, May/Jun. 1993.

[2] V. W. S. Chan, "All-Optical networks," *Scientific Amer.*, vol. 273, no. 3, pp. 56–59, Sep. 1995.

[3] "Architecture of optical transport networks," ITU, ITU-T Recommendation G. 872, 1999.

[4] V. W. S. Chan and A. H. Chan, "Reliable message delivery via unreliable networks," in *Proc. IEEE Int. Symp. Inf. Theory*, Ulm, Germany, Jun.-Jul. 29–4, 1997, p. 317.

[5] S. Parikh, "On the use of Erasure Codes in Unreliable Data Network," M.Sc. thesis, Mass. Inst. Technol., Cambridge, MA, 2001.

[6] G. Weichenberg, "High-reliability architectures for networks under stress," M.Sc. thesis, Elec. Eng. Comput. Sci. Dept., Mass. Inst. Technol., Cambridge, MA, 2003.

[7] G. E. Weichenberg, V. W. S. Chan, and M. Medard, "A reliable architecture for networks under stress," *Proc. 4th Int. Workshop Design Reliable Commun. Netw.*, pp. 263–271, Oct., 19–22 2003.

[8] I. Bar-David, "Communication under the poisson regime," *IEEE Trans. Inf. Theory*, vol. IT-15, no. 1, pp. 31–37, Jan. 1969.

[9] D. L. Snyder, *Random Point Processes*. New York: Wiley, 1975.

[10] C. W. Helstrom and R. S. Kennedy, "Noncommuting observables in quantum detection and estimation theory," *IEEE Trans. Inf. Theory*, vol. IT-20, no. 1, pp. 16–24, Jan. 1974.

[11] S. Karp and J. R. Clark, "Photon counting: A problem in classical noise theory," *IEEE Trans. Inf. Theory*, vol. IT-16, pp. 672–680, Nov. 1970.

[12] H. L. Van Trees, *Detection, Estimation and Modulation Theory*. New York: Wiley, 1968, pt. I.

[13] D. P. Bertsekas and J. N. Tsitsiklis, *Introduction to Probability*. Belmont, MA: Athena Scientific, 2002.

[14] D. P. Bertsekas, *Nonlinear Programming*, 2nd ed. Belmont, MA: Athena Scientific, 1999.

[15] S. J. Dolinar, Jr., "A class of optical receivers using optical feedback," Ph.D. dissertation, Mass. Inst. Technol., Cambridge, MA, 1976.

[16] V. W. S. Chan, "Coding for the turbulent atmospheric optical channels," *IEEE Trans. Commun.*, vol. COM-30, pp. 269–275, Jan. 1982.

[17] D. P. Bertsekas, *Dynamic Programming and Optimal Control*, 2nd ed. Belmont, MA: Athena Scientific, 2000.

Yonggang Wen (S'99) was born in Nanchang, Jiangxi, China, in 1977. He received the B.Eng. degree from the University of Science and Technology of China (USTC), Hefei, China, in 1999, and the M.Phil. degree from the Chinese University of Hong Kong (CUHK), Shatin, in 2001. Since 2001, he has been working towards Ph.D. degree in the Department of Electrical Engineering and Computer Science, Massachusetts Institute of Technology, Cambridge.

He worked from 1997 to 1999 as a Research Assistant in the Personal Communication Network and Spread Spectrum Laboratory, USTC, with much attention to the G3 mobile communication. From 1999 to 2001, he was a Research Assistant in the Lightwave Communication Laboratory, CUHK, working on optical code-division multiplexing systems and high-rate optical routing network. Currently, as a Research Assistant at the Laboratory for Information and Decision Systems, MIT, his research interests focus on mesh-based network architecture including ultra-reliable all-optical network architecture, efficient network management algorithms, and schedule over packet-based networks.

Vincent W. S. Chan (S'69–M'88–F'94) received the B.S., M.S., and Ph.D. degrees in electrical engineering, in the area of communications, from the Massachusetts Institute of Technology (MIT), Cambridge, in 1971, 1972, and 1974, respectively.

He is the Joan and Irwin Jacob Professor of Electrical Engineering and Computer Science, and Aeronautics and Astronautics, and Director of the Laboratory for Information and Decision Systems (LIDS), MIT. From 1974 to 1977, he was an Assistant Professor with the School of Electrical Engineering, Cornell University, Ithaca, NY. He joined Lincoln Laboratory, MIT in 1977 as a Staff Member of the Satellite Communication System Engineering Group working on military communications and networking. In January 1981, he became the Assistant Leader of the Communication Technology Group starting a research and development program on optical space communications. In July 1983, he formed and became Leader of the Optical Communication Technology Group and Manager of the Laser Intersatellite Transmission Experiment (LITE) Program. He became the Head of the Communications and Information Technology Division, Lincoln Laboratory until joining LIDS in 1999. He also served as the principal investigator of a Next-Generation Internet Consortium (ONRAMP) formed among AT&T, Cabletron, MIT, and JDS Fitel, and a Satellite Networking Research Consortium formed between MIT, Motorola, Teledesic, and Globalstar. He is a member of the Board of Directors of Vitesse Semiconductor Corporation and the Chairman of its Technical Advisory Board. He also serves on the Technical Advisory Boards of Agility Communications, Axiowave Networks (TAB Chairman), and as a Member of the Corporation of Draper Laboratory. His research interests are in optical communications, wireless communications, space communications and networks.

Dr. Chan is a Fellow of the Optical Society of America.